ACS Biomaterials SCIENCE & ENGINEERING

pubs.acs.org/journal/abseba

Letter

Membrane-Cloaked Nanoparticles for RNA Interference of β-Catenin in Triple-Negative Breast Cancer

Mackenzie A. Scully, Ruth Wilhelm, Dana E. Wilkins, and Emily S. Day*

Cite This: https://doi.org/10.1021/acsbiomaterials.4c00160

Read Online

ACCESS | Metrics & More | Article Recommendations | Supporting Information

ABSTRACT: There is an outstanding need for targeted therapies for triple-negative breast cancer (TNBC), an aggressive breast cancer subtype. Since TNBC's rapid growth and metastasis are driven by hyperactive Wnt signaling, suppressing the key-pathway mediator β-catenin through RNA interference may improve patient outcomes. However, small interfering ribonucleic acid (siRNA) molecules require a carrier to elicit targeted gene silencing. Here, we show that 4T1 cancer cell membrane wrapped poly(lactic-*co*-glycolic acid) (PLGA) nanoparticles (NPs) can deliver siRNA into TNBC cells, silence β-catenin expression, and reduce the cells' tumorigenic qualities. Compared to unwrapped and nontargeted NPs, the cancer cell membrane wrapped nanoparticles (CCNPs) exhibit dramatically improved uptake by TNBC cells versus breast epithelial cells and greater gene silencing at mRNA and protein levels. Congruently, β-catenin siRNA-loaded CCNPs significantly activate senescence in 2D cultured TNBC cells and reduce proliferation in 3D spheroids. This work advances the development of nucleic acid carriers for targeted RNA interference therapy.

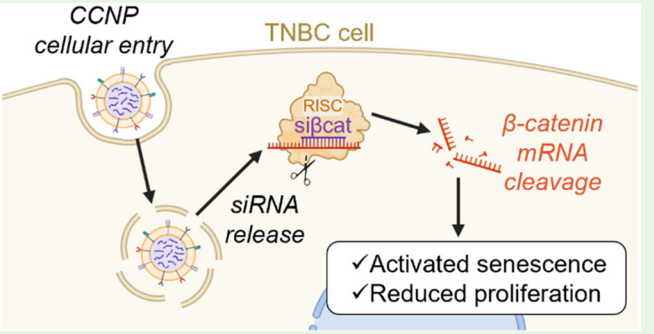

KEYWORDS: *nanomedicine, biomimetic, oncology, gene regulation, targeted therapy, membrane-wrapped, Wnt signaling, siRNA*

Triple-negative breast cancer (TNBC) accounts for 10–15% of all breast cancers and is unsusceptible to traditional hormonal- or molecular-oriented therapies because it lacks expression of the receptors that these therapies attack.[1] Consequently, patient treatment options are limited to cytotoxic chemotherapy, debilitating radiation, and invasive surgery.[2−4] Chemotherapy suffers from off-target toxicity and development of cellular resistance,[2,5] and surgery and radiation can eliminate primary tumors but not metastatic lesions.[2,6] New treatment strategies are needed to improve TNBC patient prognosis, and targeted gene regulation is a promising approach with immense potential for profound impact.

The Wnt/β-catenin signaling pathway is a desirable target for RNA interference (RNAi) due to its hyperactive behavior in TNBC (Scheme 1).[7−10] In healthy cells, Wnt signaling is a highly controlled process wherein a destruction complex continuously regulates β-catenin expression (Scheme 1A).[10] In contrast, TNBC cells overexpress transmembrane frizzled (FZD) receptors and LRP5/6 coreceptors (low-density lipoprotein receptor-related proteins 5 and 6), which are activated by extracellular Wnt ligands. Upon ligand/receptor binding, the intracellular protein dishevelled inhibits the β-catenin destruction complex, preventing β-catenin degradation (Scheme 1B).[7,10−13] Stabilized β-catenin translocates to the nucleus where it activates transcription of genes that trigger cancer cell proliferation, apoptosis evasion, dysregulated metabolism, and increased metastatic potential.[5,11,14] The critical role of β-catenin as a key mediator of TNBC growth, treatment resistance, and metastasis makes it a highly desirable target for therapeutic intervention.[8,11,14] Unfortunately, β-catenin is challenging to target with conventional small molecule drugs or monoclonal antibodies.[9,12,15] Consequently, there are no clinically approved therapies to target β-catenin directly.[9,12,13] Delivering synthetic small interfering RNA (siRNA) into diseased cells to facilitate the RNAi-mediated degradation of β-catenin messenger RNA (mRNA) is an attractive alternative strategy to silence β-catenin expression and limit disease progression. Because naked siRNA has a poor pharmacokinetic profile and limited cellular uptake,[16−18] it requires a stable delivery vehicle that can target desired cells to fulfill its therapeutic potential. We introduce one such carrier to silence β-catenin in TNBC cells.

Our carrier utilizes biomimetic nanotechnology, which is an innovative and effective approach to deliver therapeutic cargoes into diseased tissues/cells.[19,20] Prior work has shown that nanoparticles (NPs) comprised of poly(lactic-*co*-glycolic acid) (PLGA), an FDA-approved, biocompatible, and biodegradable polymer with tunable physicochemical proper-

Received: January 24, 2024
Revised: January 26, 2024
Accepted: January 30, 2024

Scheme 1. Wnt Signaling Pathway in a Healthy Cell versus TNBC Cell[a]

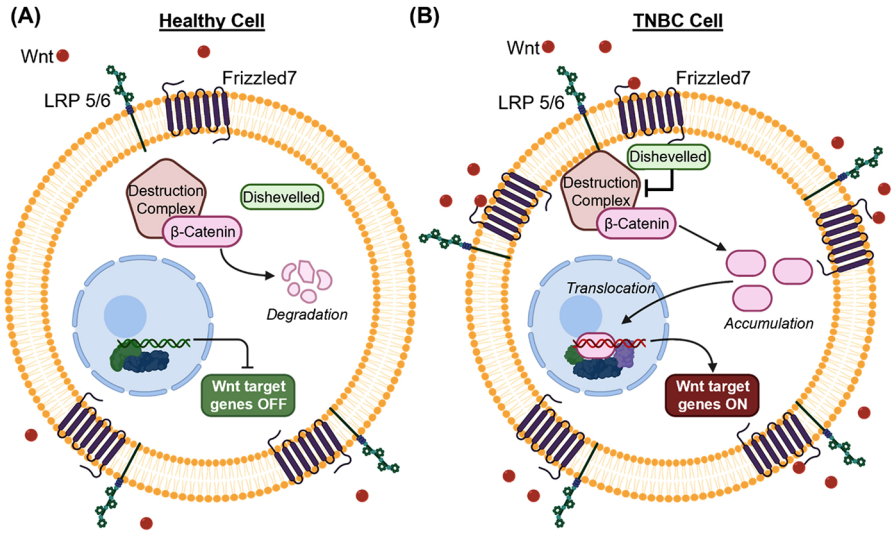

[a](A) In healthy cells, β-catenin molecules are continuously degraded by a destruction complex which controls Wnt target gene levels. (B) In TNBC cells, extracellular Wnt proteins bind overexpressed Frizzled7 and LRP5/6 coreceptors to inhibit the β-catenin destruction complex. Stabilized β-catenin accumulates in the cytoplasm, enters the nucleus, and binds transcription factors to activate Wnt target genes that drive disease progression. Created with BioRender.com.

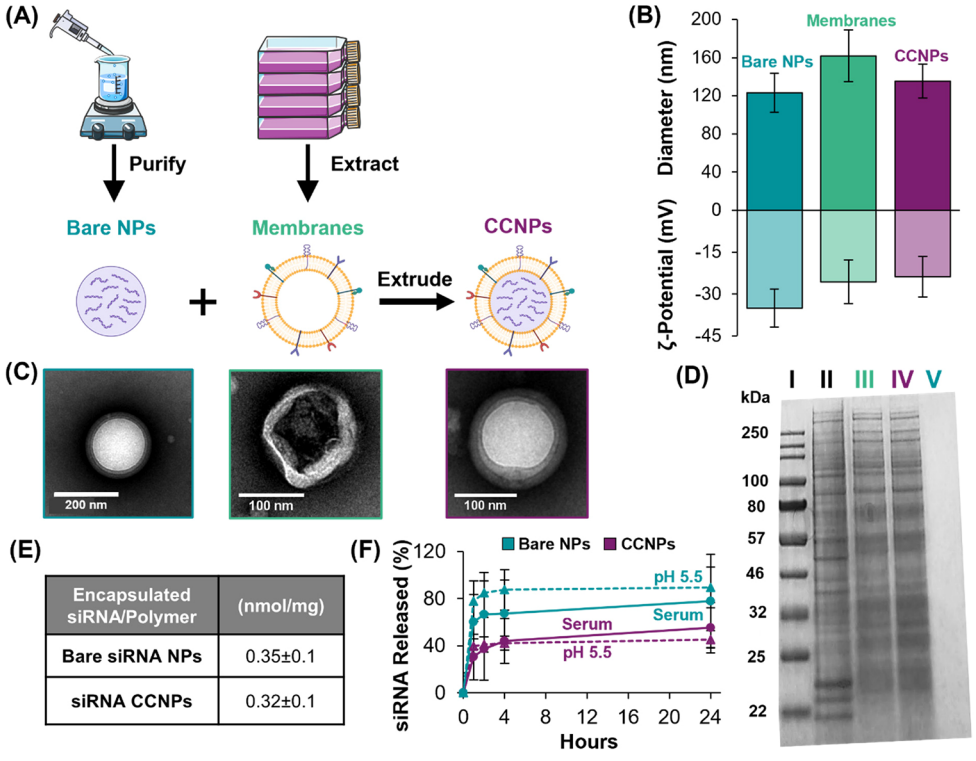

Figure 1. Synthesis and characterization of CCNPs. (A) siRNA-loaded PLGA NPs are synthesized and extruded with membrane vesicles extracted from 4T1 mammary breast cancer cells to form CCNPs. Created with BioRender.com. (B) Diameter and zeta potential of Bare NPs (n = 60), membranes (n = 42), and CCNPs (n = 45). (C) Transmission electron micrographs of all three components, with images corresponding to the scheme directly above in A. (D) SDS-PAGE gel showing (I) the known protein ladder and proteins lysed from (II) 4T1 whole cell lysate, (III) isolated 4T1 cell membrane vesicles, (IV) siRNA-loaded CCNPs, and (V) bare siRNA NPs. (E) Quantification of siRNA loading in bare PLGA NPs or CCNPs based on fluorescent analysis of Cy5-siRNA (n = 5 per group). (F) siRNA release from Bare NPs or CCNPs over 24 h in serum conditions (10% FBS, 37 °C, 100 rpm) or intracellular conditions (pH 5.5 PBS, 37 °C, 100 rpm; n = 3 per time point).

ties,[21−23] can be cloaked with cell membranes to form delivery vehicles with immune evasion and cellular targeting capabilities. Cell membrane coatings harness the complex composition of surface receptors, proteins, and phospholipids present on cell membranes to achieve effective biointerfacing.[24,25] Cancer cell membranes in particular can reduce the immune clearance and immunogenicity of coated NPs while also facilitating homotypic targeting of cancer cells throughout

https://doi.org/10.1021/acsbiomaterials.4c00160
ACS Biomater. Sci. Eng. XXXX, XXX, XXX−XXX

the body by exploiting cell adhesion processes that are naturally used for metastasis.[26−28] These capabilities are facilitated by "marker of self" and "self-recognition" molecules in the cell membrane, such as CD47 and Tf-antigen.[29,30] Previous studies have shown PLGA NPs loaded with siRNA can be coated with human cervical cancer cell membranes to treat cervical cancer, megakaryocytic cell membranes to target the hematopoietic stem and progenitor cell rich bone marrow of hematological diseases, mesenchymal stem cell membranes to treat osteosarcoma, and transformed M2 macrophage membranes to inhibit inflammation and prevent tendon adhesions.[26,31−34] siRNA has also been delivered in biomimetic nanoplatforms based on other core materials (including iron oxide and zeolitic imidazolate framework-8 (ZIF-8)-based NPs) to target prostate cancer, HER2+ breast cancer cells, or glioblastoma.[35−37] To date, biomimetic siRNA nanocarriers have not been applied to treat TNBC. TNBC is an ideal candidate for a cancer cell membrane wrapped, siRNA-loaded PLGA NP therapy, as it lacks effective targeted therapies and β-catenin offers a known molecular target for RNAi. To test this approach, we developed PLGA NPs loaded with siRNA targeting β-catenin (siβcat) and coated with TNBC membranes. We hypothesized that these cancer cell membrane-wrapped, siRNA-loaded PLGA NPs (CCNPs) would outperform unwrapped NPs and conventional siRNA-loaded poly(ethylene glycol)-PLGA (PEG−PLGA) copolymer NPs by increasing preferential uptake by targeted TNBC cells, resulting in greater inhibition of β-catenin mRNA and protein expression and effective inhibition of TNBC cellular function *in vitro*. This work advances the field by demonstrating that siRNA-loaded CCNPs can regulate the expression of an "undruggable" protein in TNBC, resulting in altered cellular senescence and spheroid forming capacity.

To make CCNPs, membranes were extracted from 4T1 cells, a murine breast cancer mimic of TNBC, using methods detailed in the Supporting Information (Figure 1A).[38] 4T1 cells were lifted from adherent culture, washed with phosphate buffered saline (PBS), and suspended in hypotonic lysis buffer on ice. The lysed cells were mechanically homogenized and subjected to differential centrifugation to remove the intracellular components. The final cell component solution was ultracentrifuged to isolate a pellet of membrane vesicles that was suspended in water. To make siRNA-loaded PLGA NPs (which were left uncoated or wrapped in cell membranes), ∼5 nmol of siRNA diluted in 100 μL of 1% poly(vinyl)-alcohol (PVA) in RNase-free water was added dropwise to PLGA dissolved in acetone at 4 mg/mL while stirring (Figure 1A). This mixture stirred for ∼3 min and was then added dropwise while stirring to 0.1% PVA. After stirring overnight, the produced NPs were isolated by centrifugal filtration. Nanoparticle tracking analysis (NTA) was used to measure the NPs' and membranes' mean diameter and concentration (particles/mL), and dynamic light scattering was used to measure zeta potential. The siRNA PLGA NPs had a mean diameter of 123.1 ± 20.3 nm and a mean charge of −35.6 ± 6.8 mV, while 4T1 membranes had a mean diameter of 161.7 ± 27.1 nm and a mean charge of −25.6 ± 7.9 mV (Figure 1B). To wrap the siRNA PLGA NPs with membranes, they were mixed in a 1:1 membrane/NP ratio (based on NTA concentration measurements) prior to mechanical extrusion through a 400 nm polycarbonate membrane (Figure 1A). The siRNA CCNPs' mean diameter and charge were 135.3 ± 17.9 nm and −23.7 ± 7.2 mV, respectively (Figure 1B). The ∼12 nm diameter increase and ∼11 mV zeta potential increase from Bare NPs to CCNPs indicate that the membrane coating was successfully formed. Transmission electron microscopy (TEM) confirmed the core−shell structure of the CCNPs (Figure 1C).

Protein content of the extracted membranes was assessed using SDS-PAGE and Western blots. Lysed proteins isolated from 4T1 whole cell lysate, extracted membranes, siβcat CCNPs, and siβcat Bare NPs at equal protein concentrations were visualized by performing SDS-PAGE and staining the gel with Simply Blue Safe Stain. The extracted membranes and siβcat CCNPs shared nearly identical protein profiles without several lower molecular weight proteins that were present in the whole cell lysate (Figure 1D). Western blot revealed that 4T1 whole cell lysate had abundant histone H3 (∼17 kDa), a nuclear protein, while extracted membranes and CCNPs did not have histone H3 present (Figure S1). Bare NPs had no proteins in their composition (Figure 1D). These results indicate that nuclear proteins can be successfully removed from whole cell lysate and that CCNPs share the same protein content as extracted membranes.

The siβcat sequence was designed based on the *Mus musculus* CTNNB1 mRNA sequence. Scrambled siRNA (siScr) was also designed and confirmed to not target any related mRNA via the NCBI database. Sequences are given in Table S1. In preliminary studies, the siβcat and siScr sequences were delivered to 4T1 cells via the commercial agent Dharmafect at 50 nM for 48 h to confirm by real-time reverse transcription quantitative polymerase chain reaction (RT-qPCR) that siβcat caused the desired β-catenin knockdown and siScr did not cause unwanted gene inhibition. These validated cargoes were loaded into PLGA NPs as described above. The siRNA loading per polymer mass (nmol/mg) was determined by loading fluorescent Cy5-tagged siRNA (i.e., Cy5-siβcat) into PLGA NPs or CCNPs and then breaking down the NPs to separate aqueous fractions containing siRNA from oil phases containing polymer. The Cy5-siβcat signal in the aqueous fraction was measured using a plate reader and compared against a standard curve of Cy5-siβcat. Bare NPs and CCNPs encapsulated 0.35 ± 0.1 or 0.32 ± 0.1 nmol siRNA per milligram of polymer, indicating minimal cargo loss during the mechanical extrusion process used to form CCNPs (Figure 1E). This corresponds to an encapsulation efficiency of approximately 56% for the Bare NPs.

As an additional control, siβcat-loaded PEG−PLGA NPs (siβcat PEG NPs) were synthesized as described in the Supporting Information to reveal any advantages siβcat CCNPs possess over a nontargeting but passivated NP design. These PEG NPs had a mean diameter of 138.4 ± 24.4 nm and a mean zeta potential of −28.7 ± 4.9 mV (Table S2). Their siRNA loading was 0.35 ± 0.2 nmol siRNA/mg polymer (Table S2; corresponding to ∼49% encapsulation efficiency), nearly equivalent to that of Bare NPs and CCNPs. This ensures reasonable comparability when evaluating each formulation's impact on TNBC cells.

The NPs' ability to maintain their size and release Cy5-siRNA was measured in storage conditions (water, 4 °C), serum conditions (10% fetal bovine serum (FBS), 37 °C, 100 rpm), and intracellular conditions (pH 5.5 PBS, 37 °C, 100 rpm) as described in the Supporting Information (Figure 1F, Figure S2). In storage conditions, CCNPs released less siRNA over 24 h than Bare NPs and PEG NPs (Figure S2A). In serum, the membrane coating on CCNPs also slowed cargo release to ∼55% over 24 h compared to ∼78% release by Bare

https://doi.org/10.1021/acsbiomaterials.4c00160
ACS Biomater. Sci. Eng. XXXX, XXX, XXX−XXX

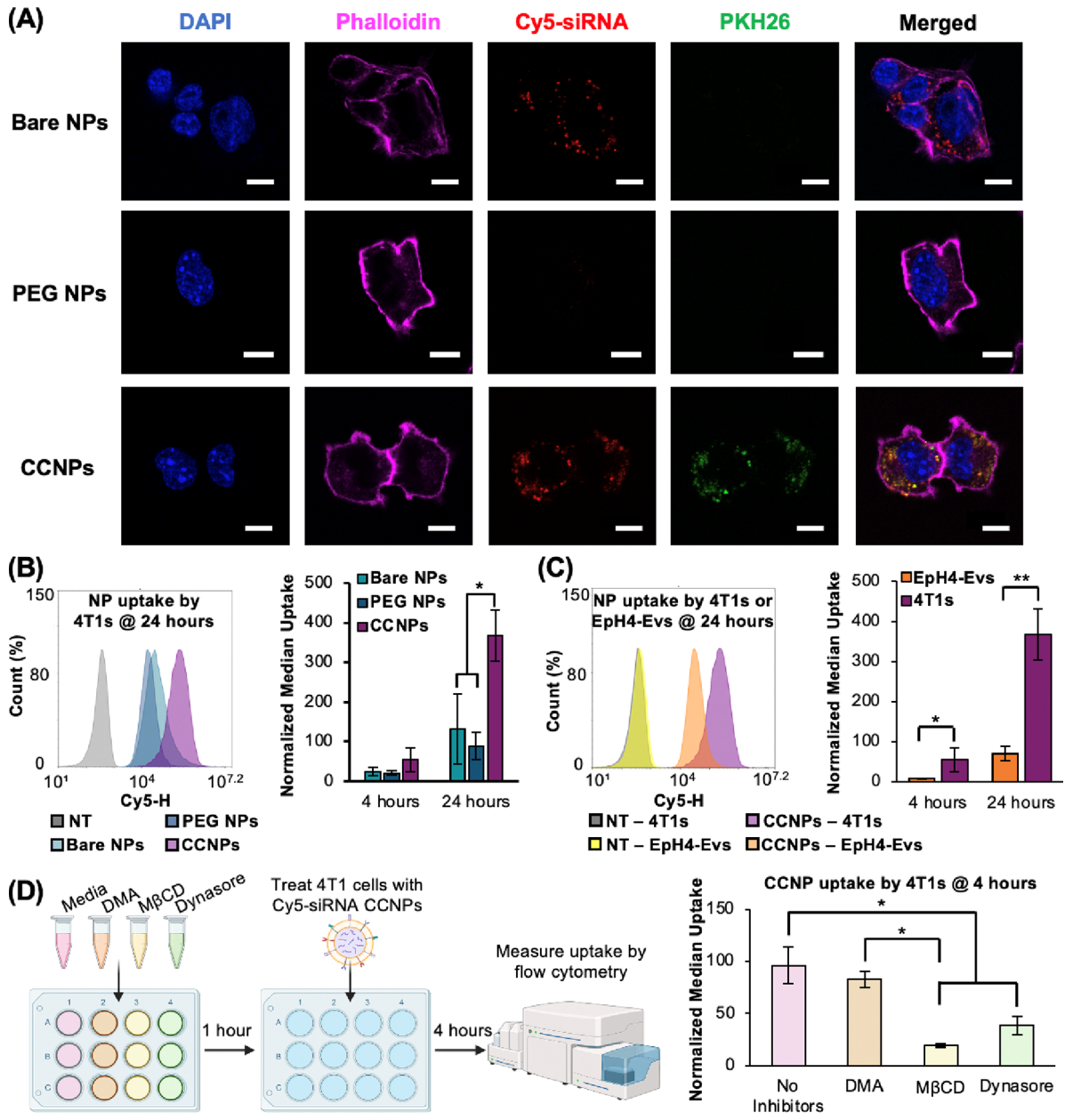

Figure 2. Cellular uptake of CCNPs and control NPs by targeted and nontargeted cells. (A) Confocal microscopy images of 4T1 cells after 24 h of incubation with Cy5-siRNA-loaded Bare NPs, PEG NPs, or CCNPs. Cell nuclei are blue (DAPI), actin is fuchsia (phalloidin), NP cargo is red (Cy5-siRNA), cell membranes on CCNPs are green (PKH26), and colocalized NP cargo and CCNP membranes are yellow. Scale bars: 10 μm. (B) (Left) Representative flow cytometry histogram and (right) median fluorescence intensity (MFI, $n = 3$) of 4T1 cells after 4 or 24 h incubation with Cy5-siRNA-loaded Bare NPs, PEG NPs, CCNPs, or saline (NT). * indicates $p < 0.05$ at 24 h by one-way ANOVA with post hoc Tukey. (C, left) Representative flow cytometry histogram and (right) MFI ($n = 3$) of EpH4-Ev epithelial or 4T1 cancer cells after 4 or 24 h of incubation with Cy5-tagged siRNA-loaded CCNPs compared to saline controls (NT). * indicates $p < 0.05$ at 4 h and ** indicates $p < 0.01$ at 24 h by Student's t test. (D, left) Schematic of endocytosis inhibitor assay in 4T1 cells pretreated with media (no inhibitors), DMA, MβCD, or Dynasore. Created with BioRender.com. (Right) MFI of Cy5-siRNA in pretreated 4T1 cells after 4 h of incubation with Cy5-siRNA-loaded CCNPs ($n = 3$). * indicates $p < 0.05$ at 4 h by one-way ANOVA with post hoc Tukey. Error bars represent standard deviation.

NPs (Figure 1F) and ~81% release by PEG NPs (Figure S2B). This is important because nanocarriers must shield siRNA during blood circulation before it is delivered into tumor cells. Under acidic intracellular conditions, CCNPs also exhibited slower siRNA release than Bare NPs (Figure 1F). Regarding size stability, CCNPs and Bare NPs exhibited similar stability in storage (Figure S2C) and serum (Figure S2D) conditions over 72 and 48 h, respectively. Under acidic intracellular conditions, both CCNPs and Bare NPs decreased in size over 48 h, indicative of NP breakdown (Figure S2E). Hence, the membrane coating slows down but does not prevent siRNA release from the NPs, making them promising nanocarriers for RNAi.

To visualize the uptake of CCNPs, Bare NPs, or PEG NPs by 4T1 murine TNBC cells, Cy5-siRNA was used as a fluorescent cargo in each particle type, and the CCNP membranes were stained with PKH26 lipophilic membrane dye. Cells were treated with NPs for 24 h, then confocal

https://doi.org/10.1021/acsbiomaterials.4c00160
ACS Biomater. Sci. Eng. XXXX, XXX, XXX−XXX

microscopy was performed to identify Cy5-siRNA (red), PKH26-labeled membranes (green), nuclei (stained with DAPI, blue), and actin (stained with Phalloidin, fuchsia; Figure 2A). CCNPs accumulated in the cytosol of 4T1 cells as evidenced by the presence of both the Cy5-siRNA signal and the PKH26 membrane signal (Figure 2A). While Cy5-siRNA was also identified in cells treated with Bare NPs, a minimal signal was observed in cells treated with PEG NPs. To quantitatively assess differences in uptake, 4T1 cells were treated for 4 or 24 h with Bare NPs, PEG NPs, or CCNPs loaded with Cy5-siβcat, and then flow cytometry was performed to measure Cy5 signal in the cells (Figure 2B). After 4 h, CCNPs had 2.6- and 2.2-times greater Cy5 signal in 4T1s compared to PEG NPs or Bare NPs, respectively (Figure 2B). After 24 h, CCNPs showed 4.2- and 2.8-times greater uptake than PEG NPs or Bare NPs, respectively (Figure 2B). This increased uptake is attributed to ligands on CCNP membranes that mediate binding to homotypic 4T1 cells. To investigate if CCNPs are preferentially internalized by 4T1 cells versus nontargeted cells, EpH4-Ev murine mammary gland epithelial cells were used as a control to mimic cells found in breast tissue surrounding tumor regions in the patient setting (representative histogram in Figure 2C). After 4 and 24 h of treatment, 4T1 cells had ~6 and ~5 times greater uptake of CCNPs, respectively, than EpH4-Ev cells, which was a statistically significant increase (Figure 2C). These results demonstrate the cancer membrane coating significantly enhances CCNP entry into targeted cells while minimizing uptake by nontargeted breast epithelial cells.

To elucidate the mechanisms CCNPs employ to enter cancer cells, we performed endocytosis inhibition assays that utilized 5-(N,N-dimethyl)-amiloride (hydrochloride) (DMA), methyl-β-cyclodextrin (MβCD), or Dynasore to block macropinocytosis, lipid raft-mediated/caveolae-mediated endocytosis, or dynamin dependent endocytosis, respectively. 4T1 cells were pretreated with each inhibitor for 1 h, dosed with Cy5-siβcat CCNPs for 24 h, then analyzed with flow cytometry (Figure 2D). Compared to cells treated with media, 4T1 cells exhibited reduced uptake of CCNPs after treatment with MβCD (~6.3× less), Dynasore (~2.9× less), and DMA (1.5× less; Figure 2D). As MβCD caused the most drastic reduction in CCNP uptake, this indicates CCNPs primarily utilize lipid-raft/caveolae-dependent mechanisms to enter 4T1 cells, though dynamin-dependent endocytosis also plays a statistically significant role.

We next evaluated CCNPs' ability to reduce β-catenin expression in 4T1 cells. The cells were treated for 48 h with 500 nM siRNA (either siScr or siβcat) delivered via Bare NPs, CCNPs, or PEG NPs. Based on the siRNA (nmol) delivered per polymer (mg), in each well of a six-well plate for a 500 nM dose of NPs, 1.43 mg of bare or PEG NPs, and 1.56 mg of CCNPs were delivered per treatment. The treatment of 500 nM siRNA delivered via NPs for 48 h was decided after dose escalation studies that tested 100, 200, or 500 nM treatments for 48 or 72 h. The lower concentrations and longer time point did not cause sufficient gene regulation, so 500 nM and 48 h were selected for subsequent experiments. A real-time reverse transcription quantitative polymerase chain reaction (RT-qPCR) revealed that, under these conditions, CCNPs significantly reduced β-catenin mRNA expression by 60% when compared to siScr Bare NPs and by 72% versus siScr CCNPs (Figure 3A). This indicates the reduced β-catenin mRNA expression is due to the delivered siβcat cargo and not

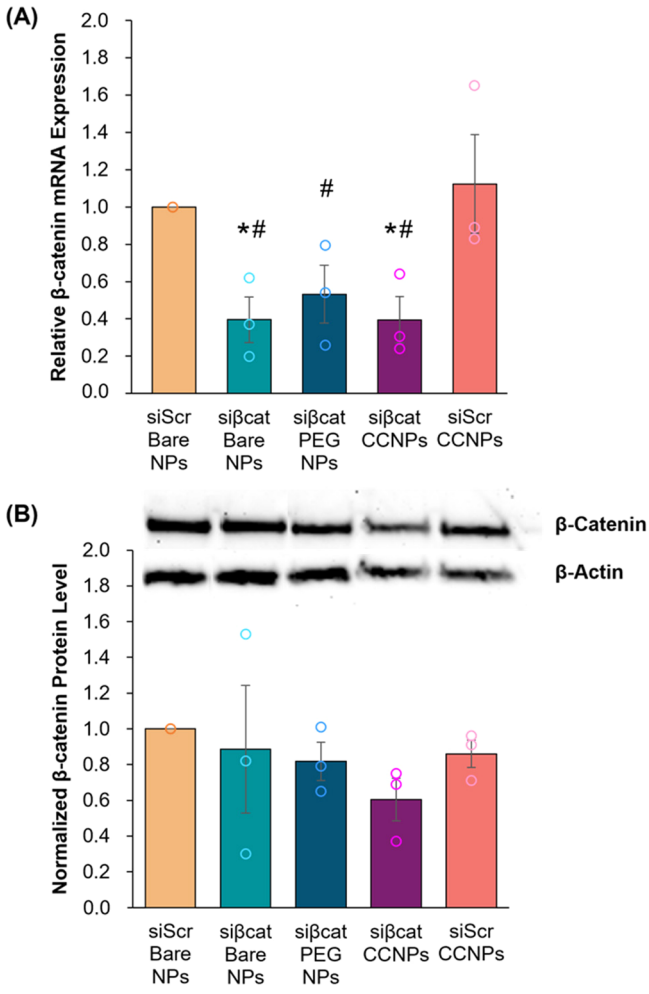

Figure 3. β-catenin mRNA and protein expression in TNBC cells treated with siRNA-loaded CCNPs and controls. (A) RT-qPCR analysis of β-catenin mRNA expression in 4T1 cancer cells treated with 500 nM siβcat loaded in Bare NPs, PEG NPs, or CCNPs or a control siScr loaded in Bare NPs or CCNPs for 48 h (n = 3). Relative mRNA expression in NP treated groups is normalized to housekeeping gene GAPDH and then normalized to cells treated with bare siScr NPs. * indicates $p < 0.05$ versus bare siScr NPs by Student's t test. # indicates $p < 0.05$ versus siScr CCNPs by Student's t test. (B) Representative Western blot showing β-catenin and β-actin protein levels in 4T1 cells treated with 500 nM siβcat loaded in Bare NPs, PEG NPs, or CCNPs or siScr loaded in Bare NPs or CCNPs for 48 h. Quasi-quantitative analysis of β-catenin protein expression from Western blots (n = 3). Expression in NP-treated cells was normalized to that in bare siScr NPs. In both A and B, colored bars indicate the group mean and open circles show individual data points. Error bars represent the standard error.

due to the siScr sequence, PLGA NP carrier, or cancer membrane exterior on CCNPs. siβcat CCNPs had similar effects on β-catenin mRNA expression as siβcat-loaded Bare NPs, which shows that the membrane coating does not inhibit intracellular siRNA activity. When 4T1 cells were treated for 48 h with 500 nM of siRNA-loaded NPs, Western blot analyses showed that siβcat CCNPs reduced β-catenin protein expression by ~40%, while siβcat Bare NPs and siβcat PEG NPs reduced protein expression by ~12% and ~18%, respectively (Figure 3B). The improved protein-level effects of siβcat CCNPs may be due to their slower siRNA release kinetics or increased cellular uptake compared with unwrapped

https://doi.org/10.1021/acsbiomaterials.4c00160
ACS Biomater. Sci. Eng. XXXX, XXX, XXX−XXX

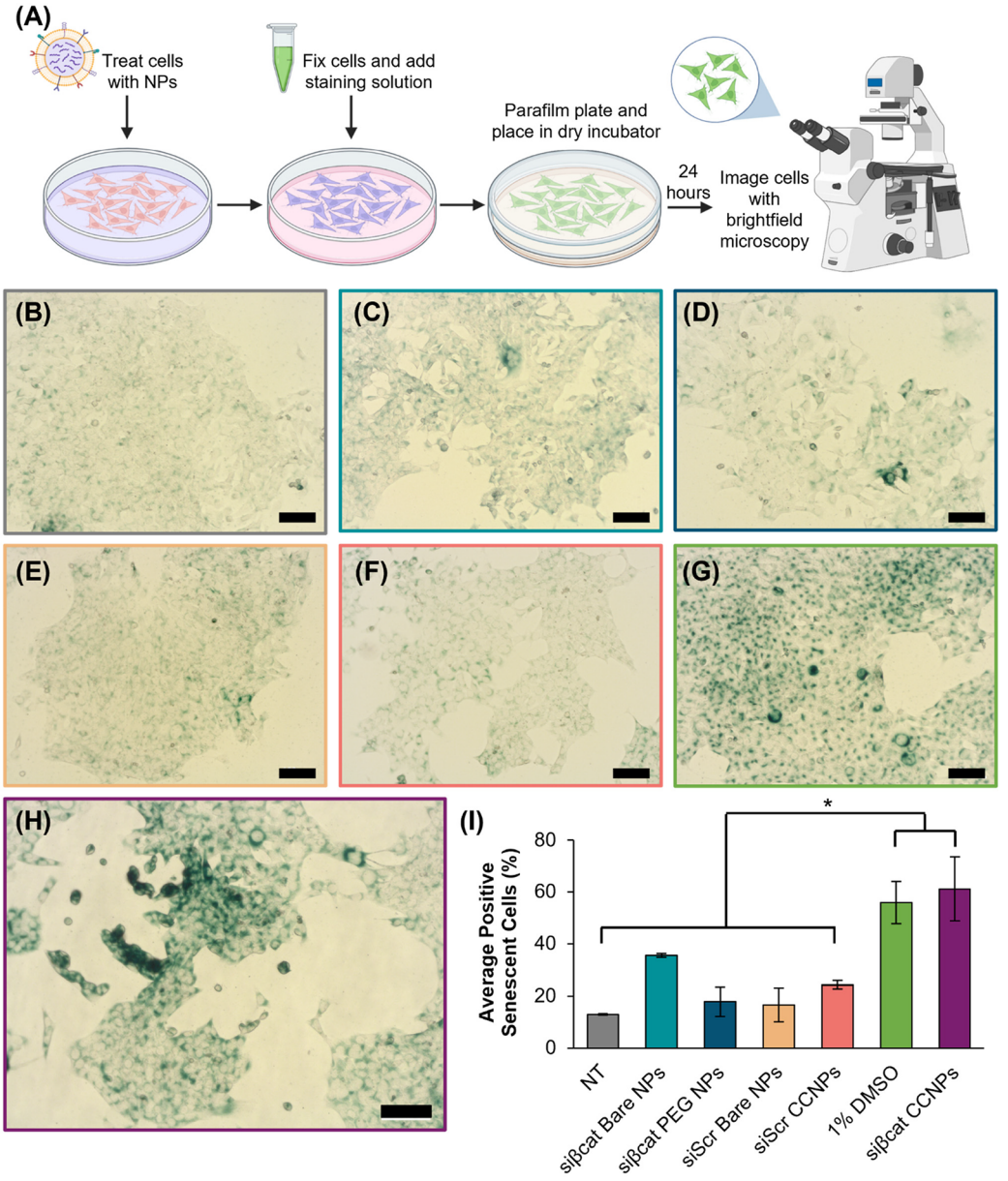

Figure 4. Effect of CCNPs loaded with siβcat on TNBC cell senescence. (A) Schematic of the senescence-associated β-galactosidase assay created with BioRender.com. Representative bright-field microscopy images of stained 4T1 cells after 48 h treatment with (B) media only (no treatment; NT), (C) siβcat Bare NPs, (D) siβcat PEG NPs, (E) siScr Bare NPs, (F) siScr CCNPs, (G) 1% DMSO (positive control), or (H) siβcat CCNPs. Teal indicates positive SAβGal staining. Scales = 100 μm. (I) Quantification of the average positive senescent cell percentage (positively stained cells/total cells in image × 100) via ImageJ analysis of microscopy images (n = 3). * indicates $p < 0.01$ versus NT, siβcat Bare NPs, siβcat PEG NPs, siScr Bare NPs, and siScr CCNPs by one-way ANOVA with post hoc Tukey. Error bars represent standard deviation.

controls. Overall, these results indicate that CCNPs have promise as siRNA delivery vehicles to provide targeted gene regulation of β-catenin in TNBC cells.

To understand the functional impact of CCNP-mediated β-catenin inhibition on TNBC cells, we investigated cellular senescence. Senescence is a state of stable cell cycle arrest that can make cancer cells resistant to growth-promoting stimuli and that prevents the replication of cells with damaged DNA therefore halting the progression of tumorigenesis and metastasis.[39] To ensure that only senescence caused by NP treatments was being measured, younger passages (<30) of cells were used to avoid unwanted replicative senescence (Hayflick limit).[39] 4T1 cells were treated with 500 nM siβcat or siScr delivered via Bare NPs, CCNPs, or PEG NPs for 48 h. A positive control of 1% DMSO was added to cells for 1 h and then removed prior to performing a senescence-associated β-galactosidase staining assay. The expression of pH-dependent β-galactosidase activity is a characteristic of senescent cells.[39] After the 48 h NP treatment, cells were washed with PBS, fixed, and stained at pH 6.0 prior to being sealed with parafilm and incubated overnight in a dry incubator (Figure 4A). After 24 h, samples were imaged using bright-field microscopy, and the average of stained positive senescent cells was quantified using thresholding in ImageJ (Figure 4B–H). Both the cells treated with siβcat CCNPs and 1% DMSO had significantly greater senescent fractions than all other controls. siβcat CCNPs yielded 61.2% senescence, which was 1.7× and 3.4× more than siβcat Bare NPs and siβcat PEG NPs, respectively

https://doi.org/10.1021/acsbiomaterials.4c00160
ACS Biomater. Sci. Eng. XXXX, XXX, XXX−XXX

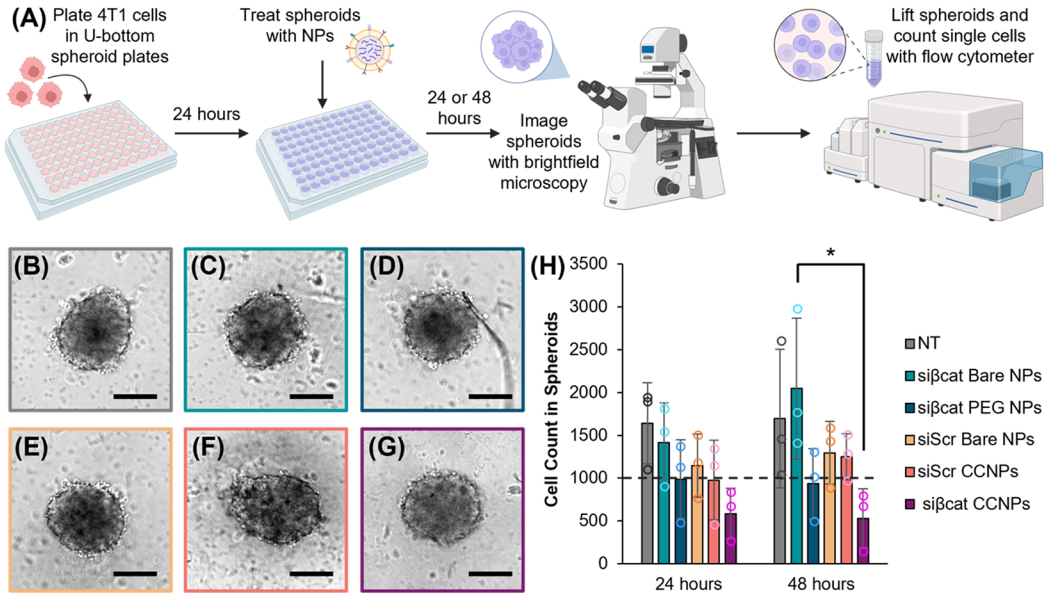

Figure 5. NP impact on spheroid formation. (A) Schematic of workflow for the spheroid formation assay. Created with BioRender.com. Brightfield images of spheroids 48 h post-treatment with (B) media only (NT), (C) siβcat Bare NPs, (D) siβcat PEG NPs, (E) siScr Bare NPs, (F) siScr CCNPs, or (G) siβcat CCNPs. Scale bar = 200 μm. Representative images of three biological replicates. (H) Cell count of spheroids using flow cytometry after 24 or 48 h of treatment with media or 500 nM siRNA loaded in Bare NPs, PEG NPs, or CCNPs (n = 3). Horizontal dashed line at 1000 indicates starting cell count for spheroid plating at 0 h. * indicates $p < 0.05$ by one-way ANOVA with post hoc Tukey. All individual data points for respective groups are plotted as open circles over the bar depicting the group mean at each time point. Error bars represent standard error.

(Figure 4I). The siScr carriers had minimal effect on senescence and were not significantly different from untreated cells (Figures 4I and S3). CCNPs' ability to significantly increase senescence in 4T1 cells further proves their potential as functional therapeutic vehicles for the RNAi of TNBC.

We also investigated CCNPs' ability to reduce tumorigenesis using a spheroid formation assay, which indicates the self-renewal potential of cancer cells (Figure 5A). We seeded 1000 4T1 cancer cells and allowed them to form spheroids overnight before treating with 500 nM siRNA delivered via Bare NPs, CCNPs, or PEG NPs. In the 96 well U-bottom plates used for spheroid formation, a 500 nM siRNA dosage was equal to about 0.286 mg of bare or PEG NPs and 0.313 mg of CCNPs per well. Spheroids were imaged using brightfield microscopy before NP treatment and at 24 and 48 h after NP treatment. Spheroids became densely packed by 48 h after treatment (Figure 5B–F), but the siβcat CCNPs reduced spheroid growth and the compacting of cells into the spheroid center, resulting in a less opaque appearance (Figure 5G) or a looser cluster of cells (Figure S4). We confirmed these qualitative assessments by lifting the spheroids and creating cell suspensions to count cells with flow cytometry (Figure 5H). At both 24 and 48 h post-treatment, siβcat CCNPs reduced the cell count compared to the controls, with the reduction being statistically significant versus siβcat Bare NPs at 48 h. These results indicate that siβcat CCNPs can release therapeutic amounts of siRNA into and throughout a spheroid's volume to reduce cell proliferation and spheroid condensation.

This work demonstrates that siRNA can be loaded within 4T1 membrane-wrapped PLGA NPs to enhance delivery to targeted TNBC cells, resulting in promising suppression of β-catenin mRNA and protein expression, leading to an onset of senescence and reduced cell proliferation to lessen spheroid formation. The improved gene silencing and therapeutic effects of CCNPs may be attributed to both their slower siRNA release kinetics in serum and intracellular conditions (Figure 1F, S2) and their substantially improved uptake by 4T1 cells (Figure 2A–C). Importantly, CCNPs exhibited minimal uptake by nontargeted breast epithelial cells (Figure 2C), indicating the membrane coating imparts specificity that reduces the risk of off-target gene silencing. Endocytosis inhibition assays indicate the CCNPs chiefly utilize lipid-raft-mediated and/or caveolae dependent mechanisms to enter TNBC cells (Figure 2D). Upon cellular uptake, CCNPs loaded with siβcat suppressed β-catenin mRNA and protein expression by 60% and 40%, respectively, outperforming both unwrapped and PEG NP controls (Figure 3A). Bare NPs or CCNPs loaded with siScr did not decrease mRNA or protein expression, indicating the carrier itself did not alter β-catenin expression (Figure 3A). Excitingly, the level of β-catenin mRNA and protein knockdown caused by siβat CCNPs was sufficient to significantly increase cellular senescence to 61.2% in a 2D culture (Figure 4I) and decrease cell proliferation in 3D breast cancer spheroids (Figure 5H). Cumulatively, these results demonstrate CCNPs can serve as successful and superior siRNA nanocarriers to enable targeted RNAi of TNBC.

These results are encouraging given the challenges associated with therapeutic manipulation of β-catenin, which is historically considered "undruggable".[40] Wnt/β-catenin signaling plays a critical role in numerous cancers, so the ability to suppress β-catenin in a targeted manner with CCNPs holds great promise as a therapeutic strategy.[9,41] Previously, CCNPs have been developed from materials including PLGA, iron oxide, metal–organic frameworks, and lipoic acid to facilitate targeted siRNA delivery, but none of these systems have targeted β-catenin or TNBC.[19] Likewise, nonbiomimetic

https://doi.org/10.1021/acsbiomaterials.4c00160
ACS Biomater. Sci. Eng. XXXX, XXX, XXX–XXX

platforms carrying siRNA against β-catenin have been fabricated from diverse materials to treat liver, colon, cervical, oral, or hepatocellular cancers[42−48] but not TNBC. Our demonstration that siRNA-loaded CCNPs can inhibit β-catenin and suppress TNBC cell function while avoiding uptake by nontargeted, healthy cells is a significant advance warranting further development of CCNPs as RNAi therapeutics for TNBC and other cancers driven by hyperactive Wnt signaling.

■ ASSOCIATED CONTENT

Supporting Information

The Supporting Information is available free of charge at https://pubs.acs.org/doi/10.1021/acsbiomaterials.4c00160.

siRNA sequences utilized (Table S1); characterization of siβcat-loaded PEG−PLGA NPs (siβcat PEG NPs; Table S2); representative Western blot protein bands for histone H3 expression in (1) 4T1 whole cell lysate, (2) 4T1 cell membranes, or (3) siβcat CCNPs (Figure S1); characterization of the siRNA release kinetics and stability of Bare NPs, PEG NPs, and CCNPs in storage or physiologic conditions (Figure S2); primer sequences used for RT-qPCR studies (Table S3); significance between treatment groups in senescence β-galactosidase assay in 4T1 cancer cells shown in Figure 4 (Figure S3); comparing NPs' impact on spheroid condensation from spheroid formation assays in Figure 5 (Figure S4) (PDF)

■ AUTHOR INFORMATION

Corresponding Author

Emily S. Day − *Department of Biomedical Engineering, University of Delaware, Newark, Delaware 19713, United States of America; Department of Materials Science and Engineering, University of Delaware, Newark, Delaware 19716, United States of America; Center for Translational Research, Helen F. Graham Cancer Center and Research Institute, Newark, Delaware 19713, United States of America;* orcid.org/0000-0002-8707-826X; Email: emilyday@udel.edu

Authors

Mackenzie A. Scully − *Department of Biomedical Engineering, University of Delaware, Newark, Delaware 19713, United States of America;* orcid.org/0000-0001-6443-4287

Ruth Wilhelm − *Department of Biomedical Engineering, University of Delaware, Newark, Delaware 19713, United States of America*

Dana E. Wilkins − *Department of Biomedical Engineering, University of Delaware, Newark, Delaware 19713, United States of America*

Complete contact information is available at: https://pubs.acs.org/10.1021/acsbiomaterials.4c00160

Author Contributions

The manuscript was written through contributions of all authors. All authors have given approval to the final version of the manuscript.

Funding

This project was supported by the National Science Foundation under grant number DMR1752009. Funding was also provided by the National Institutes of Health (NIH) under award numbers R01CA211925 and 3P20GM139760-03S1 and by the Delaware Bioscience Center for Advanced Technology. D.E.W. acknowledges support from the University of Delaware Summer Scholars Program. The content is solely the responsibility of the authors and does not necessarily represent the official views of the funding agencies.

Notes

The authors declare no competing financial interest.

■ ACKNOWLEDGMENTS

We thank S. Modla for assistance with TEM sample preparation and imaging of nanoparticles.

■ ABBREVIATIONS

TNBC, triple-negative breast cancer; siRNA, small interfering ribonucleic acid; PLGA, poly(lactic-*co*-glycolic acid); NPs, nanoparticles; CCNPs, cancer cell membrane wrapped nanoparticles; RNAi, RNA interference; FZD, frizzled receptors; LRP5/6 coreceptors, low-density lipoprotein receptor-related proteins 5 and 6; mRNA, messenger RNA; siβcat, siRNA targeting β-catenin; PEG−PLGA, poly(ethylene glycol)-PLGA copolymer; PBS, phosphate buffered saline; PVA, poly(vinyl alcohol); NTA, nanoparticle tracking analysis; TEM, transmission electron microscopy; siScr, scrambled siRNA; siβcat PEG NPs, siβcat-loaded PEG−PLGA NPs; FBS, fetal bovine serum; DMA, 5-(N,N-dimethyl)-amiloride (hydrochloride); MβCD, methyl-β-cyclodextrin; RT-qPCR, real-time reverse transcription quantitative polymerase chain reaction

■ REFERENCES

(1) Triple-negative Breast Cancer. American Cancer Society (2023). Available at: https://www.cancer.org/cancer/types/breast-cancer/about/types-of-breast-cancer/triple-negative.html (accessed: July 14, 2023).

(2) Al-mahmood, S.; Sapiezynski, J.; Garbuzenko, O. B.; Minko, T. Metastatic and triple-negative breast cancer: challenges and treatment options. *Drug Delivery Transl. Res.* **2018**, *8*, 1483−1507.

(3) Yin, L.; Duan, J.; Bian, X.; Yu, S. Triple-negative breast cancer molecular subtyping and treatment progress. *Breast Cancer Res.* **2020**, *22*, 1−13.

(4) Collignon, J.; Lousberg, L.; Schroeder, H.; Jerusalem, G. Triple-negative breast cancer: treatment challenges and solutions. *Breast Cancer Targets Ther.* **2016**, *8*, 93−107.

(5) Xu, J.; Prosperi, J. R.; Choudhury, N.; Olopade, O. I.; Goss, K. H. B-Catenin Is Required for the Tumorigenic Behavior of Triple-Negative Breast Cancer Cells. *PLoS One* **2015**, *10*, e0117097.

(6) Feys, L.; et al. Radiation-induced lung damage promotes breast cancer lung-metastasis through CXCR4 signaling. *Oncotarget* **2015**, *6*, 26615−26632.

(7) Ganesh, S.; et al. Direct pharmacological inhibition of β-catenin by RNA interference in tumors of diverse origin. *Mol. Cancer Ther.* **2016**, *15*, 2143−2154.

(8) Jang, G.-B.; Kim, J.-Y.; Cho, S.-D.; Park, K.-S.; Jung, J.-Y.; Lee, H.-Y.; Hong, I.-S.; Nam, J.-S. Blockade of Wnt/β-catenin signaling suppresses breast cancer metastasis by inhibiting CSC-like phenotype. *Sci. Rep.* **2015**, *5*, 1−15.

(9) Nusse, R.; Clevers, H. Wnt/β-Catenin Signaling, Disease, and Emerging Therapeutic Modalities. *Cell* **2017**, *169*, 985−999.

(10) Riley, R. S.; Day, E. S. Frizzled7 Antibody-Functionalized Nanoshells Enable Multivalent Binding for Wnt Signaling Inhibition in Triple Negative Breast Cancer Cells. *Small* **2017**, *13*, 1700544.

(11) Cai, J.; Guan, H.; Fang, L.; Yang, Y.; Zhu, X.; Yuan, J.; Wu, J.; Li, M. MicroRNA-374a activates Wnt/b -catenin signaling to promote breast cancer metastasis. *J. Clin. Invest.* **2013**, *123*, 566−579.

(12) Li, K.; Zhou, Z. Y.; Ji, P. P.; Luo, H. S. Knockdown of β-catenin by siRNA influences proliferation, apoptosis and invasion of the colon cancer cell line SW480. *Oncol. Lett.* **2016**, *11*, 3896−3900.
(13) Ganesh, S.; et al. RNAi-Mediated B-Catenin Inhibition Promotes T Cell Infiltration and Antitumor Activity in Combination with Immune Checkpoint Blockade. *Mol. Ther.* **2018**, *26*, 2567−2579.
(14) Dey, N.; Barwick, B. G; Moreno, C. S; Ordanic-Kodani, M.; Chen, Z.; Oprea-Ilies, G.; Tang, W.; Catzavelos, C.; Kerstann, K. F; Sledge, G. W; Abramovitz, M.; Bouzyk, M.; De, P.; Leyland-Jones, B. R Wnt signaling in triple negative breast cancer is associated with metastasis. *BMC Cancer* **2013**, *13*, 1−15.
(15) Griffiths, C. L.; Olin, J. L. Triple negative breast cancer: A brief review of its characteristics and treatment options. *J. Pharm. Pract.* **2012**, *25*, 319−323.
(16) Kanasty, R.; Dorkin, J. R.; Vegas, A.; Anderson, D. Delivery materials for siRNA therapeutics. *Nat. Mater.* **2013**, *12*, 967−977.
(17) Kim, H. J.; Kim, A.; Miyata, K.; Kataoka, K. Recent progress in development of siRNA delivery vehicles for cancer therapy. *Adv. Drug Delivery Rev.* **2016**, *104*, 61−77.
(18) Whitehead, K. A.; Langer, R.; Anderson, D. G. Knocking down barriers: Advances in siRNA delivery. *Nat. Rev. Drug Discovery* **2009**, *8*, 129−138.
(19) Scully, M. A.; Sterin, E. H.; Day, E. S. Membrane-wrapped nanoparticles for nucleic acid delivery. *Biomater. Sci.* **2022**, *10*, 4378−4391.
(20) Aboeleneen, S. B.; Scully, M. A.; Harris, J. C.; Sterin, E. H.; Day, E. S. Membrane-wrapped nanoparticles for photothermal cancer therapy. *Nano Converg.* **2022**, *9*, 1−27.
(21) Astete, C. E.; Sabliov, C. M. Synthesis and characterization of PLGA nanoparticles. *J. Biomater. Sci. Polym. Ed.* **2006**, *17*, 247−289.
(22) Vasir, J. K.; Labhasetwar, V. Biodegradable Nanoparticles for Cytosolic Delivery of Therapeutics. *Adv. Drug Delivery Rev.* **2007**, *59*, 718−728.
(23) Kumari, A.; Yadav, S. K.; Yadav, S. C. Biodegradable polymeric nanoparticles based drug delivery systems. *Colloids Surfaces B Biointerfaces* **2010**, *75*, 1−18.
(24) Fang, R. H.; Kroll, A. V.; Gao, W.; Zhang, L. Cell Membrane Coating Nanotechnology. *Adv. Mater.* **2018**, *30*, 1−34.
(25) Kroll, A. V.; Fang, R. H.; Zhang, L. Biointerfacing and applications of cell membrane-coated nanoparticles. *Bioconjugate Chem.* **2017**, *28*, 23−32.
(26) Chen, M. M.; Chen, M. M.; He, J. Cancer cell membrane cloaking nanoparticles for targeted co-delivery of doxorubicin and PD-L1 siRNA. *Artif. Cells, Nanomedicine, Biotechnol.* **2019**, *47*, 1635−1641.
(27) Sun, H.; et al. Cancer-Cell-Biomimetic Nanoparticles for Targeted Therapy of Homotypic Tumors. *Adv. Mater.* **2016**, *28*, 9581−9588.
(28) Zhu, J. Y.; et al. Preferential Cancer Cell Self-Recognition and Tumor Self-Targeting by Coating Nanoparticles with Homotypic Cancer Cell Membranes. *Nano Lett.* **2016**, *16*, 5895−5901.
(29) He, Z.; Zhang, Y.; Feng, N. Cell membrane-coated nanosized active targeted drug delivery systems homing to tumor cells : A review. *Mater. Sci. Eng., C* **2020**, *106*, 110298.
(30) Xu, C. H.; et al. Cell membrane-camouflaged nanoparticles as drug carriers for cancer therapy. *Acta Biomater.* **2020**, *105*, 1−14.
(31) Xu, C.; Liu, W.; Hu, Y.; Li, W.; Di, W. Bioinspired tumor-homing nanoplatform for co-delivery of paclitaxel and siRNA-E7 to HPV-related cervical malignancies for synergistic therapy. *Theranostics* **2020**, *10*, 3325−3339.
(32) Das, S.; et al. Megakaryocyte membrane-wrapped nanoparticles for targeted cargo delivery to hematopoietic stem and progenitor cells. *Bioeng. Transl. Med.* **2023**, *8*, 1−17.
(33) Zhao, J.; Mu, X.; Hou, X.; Zhang, X.; Li, P.; Jiang, J. Synergistic treatment of osteosarcoma with biomimetic nanoparticles transporting doxorubicin and siRNA. *Front. Oncol.* **2023**, *13*, 1−12.
(34) Sun, J.; Ju, F.; Jin, J.; Wang, H. L.; Li, Z. J.; Sun, Y. C.; Chen, Q. Z.; Yang, Q. Q.; Tan, J.; Zhou, Y. L. M2 Macrophage Membrane-Mediated Biomimetic-Nanoparticle Carrying COX-siRNA Targeted Delivery for Prevention of Tendon Adhesions by Inhibiting Inflammation. *Small* **2023**, *19*, 1−17.
(35) Mu, X.; et al. siRNA Delivery with Stem Cell Membrane-Coated Magnetic Nanoparticles for Imaging-Guided Photothermal Therapy and Gene Therapy. *ACS Biomater. Sci. Eng.* **2018**, *4*, 3895−3905.
(36) Zhuang, J.; Gong, H.; Zhou, J.; Zhang, Q.; Gao, W.; Fang, R. H.; Zhang, L. Targeted gene silencing in vivo by platelet membrane-coated metal-organic framework nanoparticles. *Sci. Adv.* **2020**, *6*, DOI: 10.1126/sciadv.aaz6108
(37) Li, Y.; et al. Macrophage − Cancer Hybrid Membrane-Camouflaged Nanoplatforms for HIF-1 α Gene Silencing-Enhanced Sonodynamic Therapy of Glioblastoma. *ACS Appl. Mater. Interfaces* **2023**, *15*, 31150−31158.
(38) Kroll, A. V.; Fang, R. H.; Jiang, Y.; Zhou, J.; Wei, X.; Yu, C. L.; Gao, J.; Luk, B. T.; Dehaini, D.; Gao, W.; Zhang, L. Nanoparticulate Delivery of Cancer Cell Membrane Elicits Multiantigenic Antitumor Immunity. *Adv. Mater.* **2017**, *29*, 1−9.
(39) Cellular Senescence. Cell Signaling Technology. Available at: https://www.cellsignal.com/science-resources/overview-of-cellular-senescence. (Accessed: July 6, 2023).
(40) Watanabe, K.; Dai, X. Winning WNT: Race to Wnt signaling inhibitors. *Proc. Natl. Acad. Sci. U. S. A.* **2011**, *108*, 5929−5930.
(41) Anastas, J. N.; Moon, R. T. WNT signalling pathways as therapeutic targets in cancer. *Nat. Rev. Cancer* **2013**, *13*, 11−26.
(42) Dudek, H.; et al. Knockdown of β-catenin with dicer-substrate siRNAs reduces liver tumor burden in vivo. *Mol. Ther.* **2014**, *22*, 92−101.
(43) Rudzinski, W. E.; Palacios, A.; Ahmed, A.; Lane, M. A.; Aminabhavi, T. M. Targeted delivery of small interfering RNA to colon cancer cells using chitosan and PEGylated chitosan nanoparticles. *Carbohydr. Polym.* **2016**, *147*, 323−332.
(44) Yu, Q.; et al. Mesoporous titanium dioxide nanocarrier with magnetic-targeting and high loading efficiency for dual-modal imaging and photodynamic therapy. *J. Mater. Chem. B* **2017**, *5*, 6081−6096.
(45) Ma, C.; et al. Nanoparticle delivery of Wnt-1 siRNA enhances photodynamic therapy by inhibiting epithelial-mesenchymal transition for oral cancer. *Biomater. Sci.* **2017**, *5*, 494−501.
(46) Matsuda, A.; Ishiguro, K.; Yan, I. K.; Patel, T. Extracellular Vesicle-Based Therapeutic Targeting of β-Catenin to Modulate Anticancer Immune Responses in Hepatocellular Cancer. *Hepatol. Commun.* **2019**, *3*, 525−541.
(47) Yan, L.; et al. Small interfering RNA-loaded chitosan hydrochloride/carboxymethyl chitosan nanoparticles for ultrasound-triggered release to hamper colorectal cancer growth in vitro. *Int. J. Biol. Macromol.* **2020**, *162*, 1303−1310.
(48) Ishiguro, K.; Yan, I. K.; Lewis-Tuffin, L.; Patel, T. Targeting Liver Cancer Stem Cells Using Engineered Biological Nanoparticles for the Treatment of Hepatocellular Cancer. *Hepatol. Commun.* **2020**, *4*, 298−313.

https://doi.org/10.1021/acsbiomaterials.4c00160
ACS Biomater. Sci. Eng. XXXX, XXX, XXX−XXX